Available online at www.sciencedirect.com

ScienceDirect

journal homepage: www.elsevier.com/locate/bbe

Review Article

On ultrasound classification of stroke risk factors from randomly chosen respondents using non-invasive multispectral ultrasonic brain measurements and adaptive profiles

Miroslaw Wrobel [a,*], *Andrzej Dabrowski* [a], *Adam Kolany* [a], *Anna Olak-Popko* [b], *Robert Olszewski* [c], *Pawel Karlowicz* [d]

[a] *SoNovum AG, Leipzig, Germany*
[b] *MTZ Clinical Research, Warsaw, Poland*
[c] *Department of Cardiology and Internal Medicine, Military Institute of Medicine, Warsaw, Poland*
[d] *Sonomed Sp. Z o. o., Warsaw, Poland*

ARTICLE INFO

Article history:
Received 11 March 2015
Received in revised form
1 July 2015
Accepted 10 October 2015
Available online 24 October 2015

Keywords:
Ultrasounds
Dispersion
Brain
Atrial fibrillation
Stroke

ABSTRACT

In this paper, we present a new brain diagnostic method based on a computer aided multispectral ultrasound diagnostics method (CAMUD). We explored the standard values of the relative time of flight (RIT), as well as the attenuation, ATN, of multispectral longitudinal ultrasound waves propagated non-invasively through the brains of a standard Caucasian volunteer population across different ages and genders. For the interpretation of the volunteers health questionnaire and ultrasound data we explored various clustering and classification algorithms, such as PCA and ANOVA. We showed that the RIT and ATN values provide very good estimators of possible physiological changes in the brain tissue and can differentiate the possible high-risk groups obtained by other groups and methods (Russo et al. [1]; Lloyd-Jones et al. [2]; Medscape [3]).

Special attention should be given to the subgroup which included almost 39% of the volunteers. Respondents in this group have a significantly increased minimum ATN value (see Classification Trees). These values are strongly correlated with the identified risk of stroke factors being: age, increased alcohol consumption, cases of heart disease and stroke in the family as already shown by Rusco and as incorporated into Lloyd-Jones et al., ''Heart Disease and Stroke Statistics – 2009 Update'', by the American Heart Association (AHA) and American Stroke Association (ASA), as updated recently in the 2015 ''Stroke Prevention Guidelines''.

* *Corresponding author at*: SoNovum AG, Leipzig, Germany.
E-mail address: miroslaw.wrobel@sonovum.de (M. Wrobel).

http://dx.doi.org/10.1016/j.bbe.2015.10.004

1. Introduction

1.1. Aim and methodology

1.1.1. Aim

Currently, scientific advances in medical diagnostic imaging such as magnetic resonance imaging (MRI), computed tomography (CT) or even ultrasound, have reached very high standards. These technologies provide comprehensive geometrical information about a patient's internal tissue structure but contain little information about its bio-chemical composition. On the other hand, laboratory analysis of biological and chemical components of a patient's blood, cerebrospinal fluid (CSF) or brain tissue provides very good information about the composition of all single substances, for instance by using chromatography, but not about the tissue structure. Furthermore, many brain tissue pathologies are often difficult to detect with standard medical imaging as those minor changes in the brain tissue do not show any discrepancies in picture that was taken. A good diagnosis, in the early phases of such brain disorders, can only be made by a very experienced specialist, such as a neurologist or psychiatrist, who can interpret a patient's initial symptoms. Unfortunately, similar to mental health problems, other brain illnesses such as traumatic brain injuries are hard to detect or to track with standard imaging or bio-chemical analysis. On the one hand, these are often too minor to occur on the single image, and on the other hand, they are too fast for chemical analysis, thus making it difficult to treat them effectively.

To overcome the shortcomings of brain diagnostic technologies that exist today, this paper will present a novel concept called ''computer aided multispectral ultrasound diagnostics'' (CAMUD) for brain health monitoring. Our solution use longitudinal mechanical ultrasound waves with frequencies in the range of lower MHz and incorporates the following components:

1. Proprietary multispectral ultrasound brain scanner SONOVUM ULTRAEASY™ [6];
2. Innovative form of brain health data analytics; and
3. Machine-learning prediction tool to diagnose, prevent possible brain impairment with early detection and to track brain disorder conditions and treatment in real time.

The first two steps will be described and discussed in detail in this paper. The third step will form the basis of a corresponding research study and the results will be presented in a subsequent paper.

The first application to employ ultrasonic methods to examine the brain relied on a simple echo reflection method. Echoencephaloscopes, devices that employ reflected ultrasonic waves to examine the position of brain structures, allowing mainly for the diagnosis of the asymmetry of anatomical structures, based on echo presented in ''A Mode'' (amplitude presentation), were created in the mid-1960s. The first Polish echoencephaloscope was developed in 1966 at the Institute of Fundamental Technological Research, Polish Academy of Sciences, under the direction of Professor Filipczynski. Successive ultrasound brain diagnostic methods like transcranial Doppler (TCD) and scanning (ultrasonography) have been widely adopted in practice. The first experiments involving a transcranial ultrasound densitometry system were made by Prof. Roman Mazur back in 2000 and published in «Udar Mózgu» [4]. The ultrasound system used in this clinical experiment examined 62 patient's brain tissue with only one frequency. The authors interpreted the recorded changes in the ultrasound signal as simple density changes of the brain tissue due to absence of blood, its hydrolyze or edema. We will demonstrate that using multiple frequencies will show the dispersive character of the brain tissue and provide some other interpretation to the signal changes. In non-linear material, as, for example biological tissue and especially human brain tissue, an effect of longitudinal wave dispersion can be clearly observed and measured. It is such effect, in which the non-linear frequency-dependent mediums bulk modulus results in different propagation speeds for different ultrasound frequencies [6]. In addition to the observed changes in propagation speed, different attenuation profiles can also be observed. Interdependence between wave speed and attenuation is in accordance with Kramers–Kronig equations ([5], (29)) where it is shown among others that

$$\frac{1}{c_2}-\frac{1}{c_1}=-\frac{2}{\pi}\cdot\int_{\omega_1}^{\omega_2}\frac{\alpha(\omega)}{\omega^2}\mathrm{d}\omega \tag{1}$$

where c_1, c_2 are propagation velocities for waves with circular frequencies ω_1 and ω_2, respectively, and $\alpha(\omega)$ is the attenuation for wave with circular frequency ω. The above, after introducing $\omega = 2\pi \cdot f$, $\omega_1 = 2\pi \cdot f_1$ and $\omega_2 = 2\pi \cdot f_2$, takes the form of:

$$\frac{1}{c_2}-\frac{1}{c_1}=-\frac{1}{\pi^2}\cdot\int_{f_1}^{f_2}\frac{\alpha(f)}{f^2}\mathrm{d}f \tag{2}$$

As will be presented further in this paper, such pattern of frequency-dependent attenuations and the corresponding propagation speeds can be used to identify the state of a medium or to track possible changes to the brain tissue in real time.

To fulfill the paper's goals, a ''SONOVUM ULTRAEASY™)'' [6] ultrasound system for data acquisition was built by E3-Technology, SONOMED and SONOVUM and used for multispectral signal collection. Data was collected by MTZ Clinical Research Warsaw (MTZ), during the medical experiment approved by Bioethics Committee Vote Reg. No. KB/916/14 (Bioethics Board Resolution no. 07/14 of the District Physicians Chamber in Warsaw from March 13, 2014) from almost 250 volunteers with representative ages and gender (see Fig. 1).

1.1.2. Experimental procedure

The collection of the ultrasound data, conducting the medical examination, and administering the volunteers' questionnaire, was performed by MTZ according to the approved protocol. The duration of the entire procedure for each healthy volunteer did not exceed 20 min. It consisted of three steps:

(A) Preparation for the main ultrasound examination

- Volunteer identification and signing informed consent.
- Answering the questionnaires (described below).

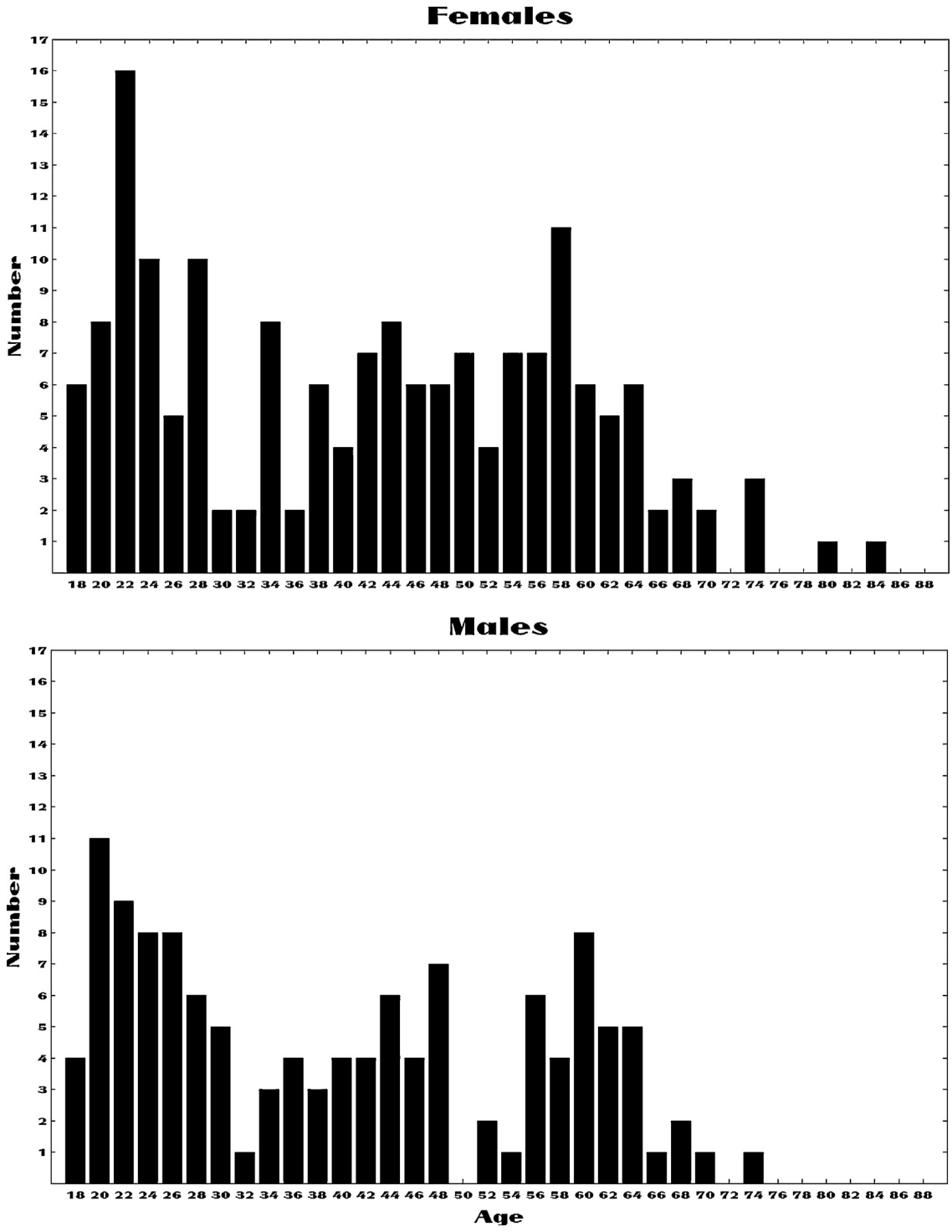

Fig. 1 – Gender/age distribution in the sample: the height of a bar represents the number of probants with the considered gender in the given age (indicated on the horizontal axis).

- Medical examination – to qualify only healthy subjects for the experiment.
- Volunteers took off all objects that could hinder putting on the measurement band and fixing the transmitter (e.g. glasses, hair bands, clips, etc.).

(B) Main ultrasound measurement

- Measurement was made in a horizontal position.
- The measurement alone took around 5 min; volunteers remained in horizontal position with their eyes closed and in relaxed condition.

- Any movements, such as yawning, chewing or swallowing were not allowed.
- Relaxing music was provided during the whole measurement session.

(C) Closing the measurement

- After taking the measurement, the unique identification code of each volunteer was set as used in the database.
- All the data was recorded and saved in the database.

One of the important components of this study was the patient's questionnaire where some additional information was acquired that we then used for classifying the sub-groups. All of the questions were designed to be based on the Heart Disease and Stroke Statistics – 2009 Update and was divided into four subsets:

1. Personal data where the standard information collected included race, gender, age, weight, height, education (primary, middle, higher);
2. Health activity including questions regarding smoking (what and how much per week – may be in packs of cigarettes), alcohol (e.g. beer, wine, vodka, none, seldom, medium, often – e.g. per week), physical activity (as in amount and type of exercise (e.g. cycling, walking) and general question such as: ''Are you interested in the state of your health?'');
3. General health condition informations, such as blood pressure, known heart and vascular diseases, diabetes, asthma or other lung diseases and blood values; as well as
4. Family information questions, such as ''Was there a stroke in the family and who had it?'' ''Did anybody in one's near family have any other cranial problems?''

1.1.3. *Methodology*

The entire procedure for acquiring data consisted of two stages:

1. A coarse approximation of frequency attenuation distribution, FAD, which consists in emitting a sequence of ultrasonic monospectral signals with in advance fixed frequencies $G = \{G_1, \ldots, G_{HFAD}\}$ and receiving their echoes. This is the basis for estimating the distribution of the attenuation of ultrasonic waves in the frequency range under consideration. As a result of that for each of the respondents a row of attenuation coefficients $\alpha_1, \ldots, \alpha_{HFAD}$ was obtained (see Fig. 2). Their values will be later referred to as ATN. In estimating the attenuation coefficients the characteristics of the measuring device was taken under consideration.
2. Emitting a profiled ultrasonic multispectral signal (see Fig. 3) whose parameters (number of frequencies HPRF and their values $F = \{F_1, \ldots, F_{HPRF}\}$ and amplitudes) were established on base of earlier made experiments. The phase shifts of individual frequency components have been chosen according to specific optimalization criteria on absolute values of peaks, their spread and the average value of the signal. The received echo is further decomposed into single frequency components acquiring the bunch of amplitude and phase value pairs (phase vectors), each for every frequency $f \in F$ with use of the well known least square method [16,17]. Afterwards a sequence of derived parameters (relative arrive times (RAT)) $T_1^{(R)}, \ldots, T_{HPRF-1}^{(R)}$ were obtained:

$$T_h^{(R)} = \frac{(F_{h+1}/c_{h+1}) - (F_h/c_h)}{\Delta F_h} \cdot \ell = T_x - \left[\Theta_h + \frac{\mathrm{mod}(\Delta\varphi_h, 2\pi)}{\Delta F_h}\right] \quad (3)$$

were obtained:where c_{h+1}, c_h are phase velocities of consecutive frequencies F_{h+1} and F_h, ℓ is the acoustic length (head diameter), $\Delta\varphi_h = \varphi_{h+1} - \varphi_h$ is the difference between phases for F_{h+1} and F_h, T_x is the time point of the measurement and Θ_h is an unknown parameter which is being estimated from observed evolution of the values:

$$\frac{\mathrm{mod}(\Delta\varphi_h, 2\pi)}{\Delta F_h} \quad (4)$$

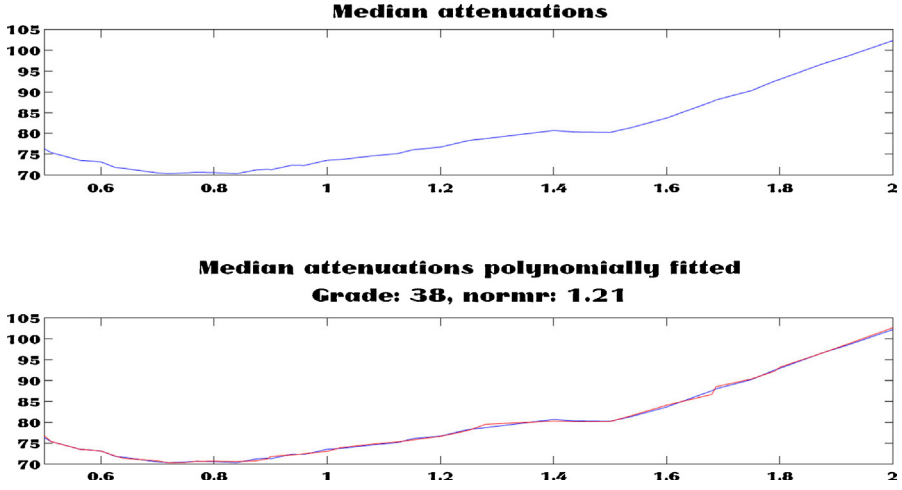

Fig. 2 – Attenuation distribution in the sample: the upper plot shows attenuations of various frequencies in the range 0.5–2.0 MHz averaged by all probants. The lower plot shows the best fitting polynomial interpolating these values.

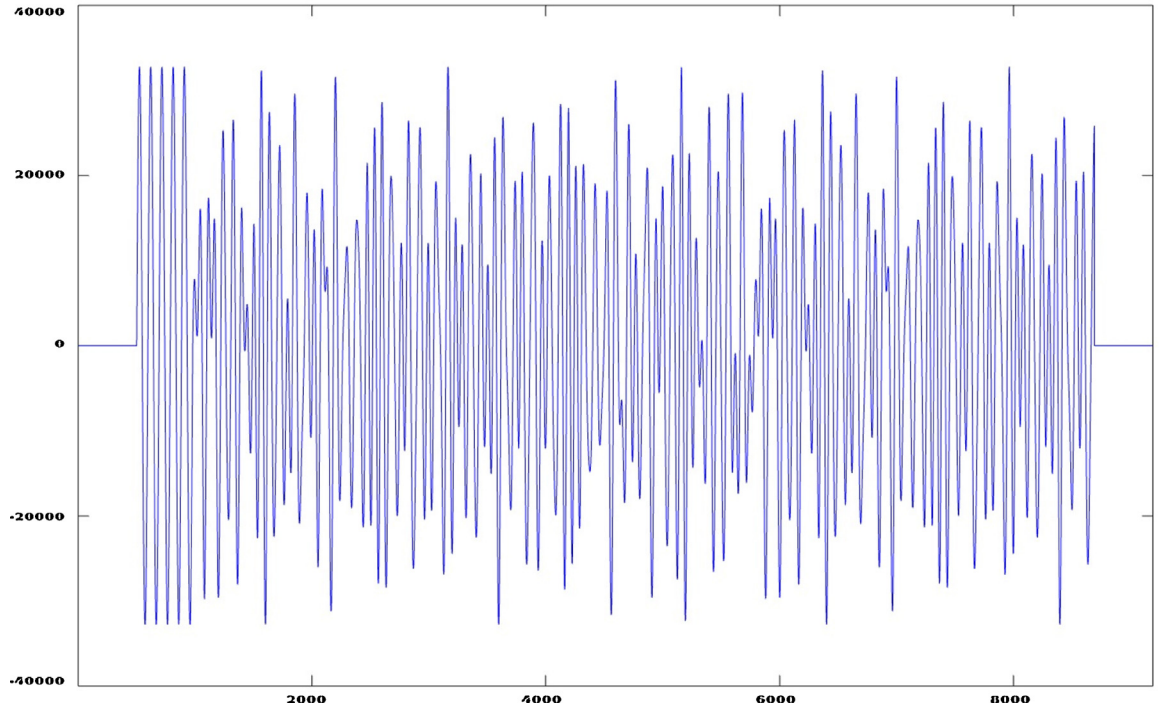

Fig. 3 – The plot of a profiled signal which consists of a superposition of 10 frequencies sampled with 96 MHz sampling frequency and a synchronization trailer (burst) at the beginning. The signal is internally represented as a sequence of *int16* values (integers in $\langle -32768, 32767 \rangle$). The burst consists of 480 elements and its values are $\sin(2\pi \cdot (n/96))$, $n = 0, \ldots, 479$ (5 periods of sampled 1 MHz sinus sequence). The length of the entire signal is $2^{13} = 8192$.

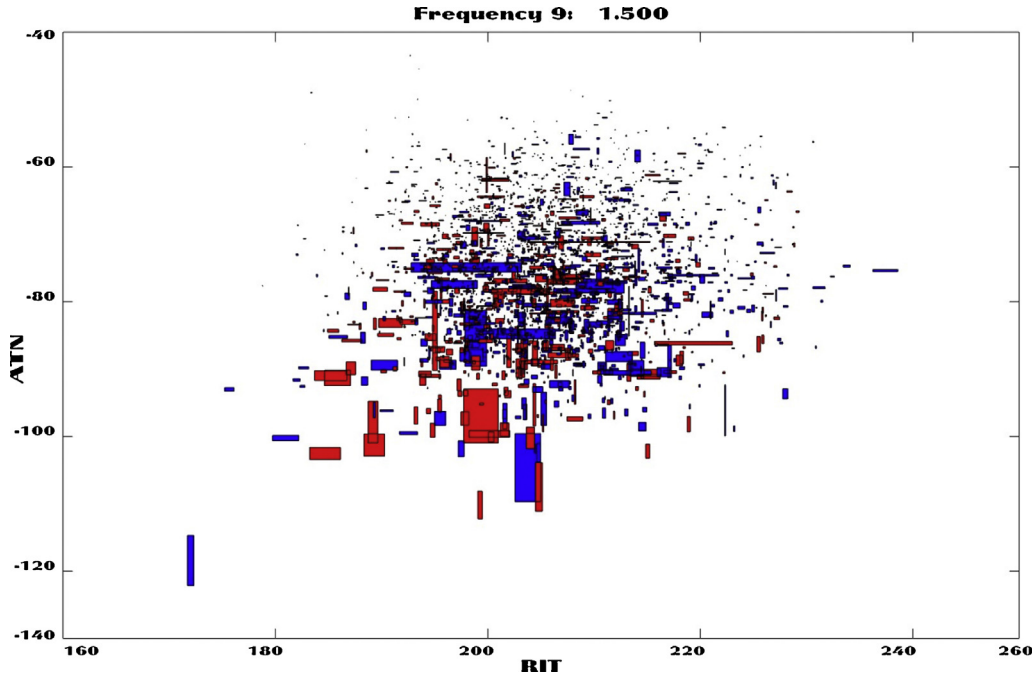

Fig. 4 – RIT/ATN correspondence: each rectangle represents a fixed individual. The color represents gender (red – female, blue – male). The left (bottom) edge of each rectangle is the first quantile of RIT (ATN) and the right (upper) edge is the third quantile of these parameters.

In case of no dispersion (wave velocity does not depend on the frequency) the values $T_h^{(R)}$ are all equal to the time T_A the wave head needs to reach the receiver after being sent (the time of arrive, ToA). In order not to consider the pure technical parameter T_x in further investigation, we restrict ourselves to parameters

$$RiT_h = \Theta_h + \frac{\mathrm{mod}(\Delta\varphi_h\,,\,2\pi)}{\Delta F_h} \tag{5}$$

with Θ_h described above and which, in case of no dispersion, is the time the wave "waits" at the receiver until being detected and which will be referred to as relative idle time (RiT). These values along with the attenuation coefficients ATN are further used for classification of investigated respondents.

2. Statistical analysis

2.1. Data collection

All the data necessary for this research was acquired by MTZ in accordance with an approved procedure. After collecting some personal data (age, gender, state of health, habits, etc.) a volunteer was subjected to an ultrasonic measurement out of which 10 complex timeseries were obtained – 1 series for 1 of 10 frequencies. These timeseries, after being decomposed into amplitudes and phase timeseries were transformed into attenuations (ATN) and relative idle times (RIT) (see Fig. 4). The latter augmented with measurement quality information are referred to as RITx.

2.2. Classification of ATN, RIT and RITx measurements

2.2.1. Dimension reduction

2.2.1.1. *Data*. The measurements (ATN, RIT and RITx with their amplitudes) are registered in a three dimensional data matrix. The dimensions are:

- frequencies (38 variables for FAD data, 9×2 variables for profile data),
- cases (247 different persons),
- repetitions (50 repetitions for FAD data, approximately 1800 profile repetitions per person).

The first reduction transforms the measurements into a two dimensional matrix. The repetitions for each frequency and each person are substituted by three quartiles (25%, 50% and 75% quantiles of distribution). The reduced data matrix is two dimensional. The columns of the data represent frequencies (38×3 variables for hat data, $9 \times 2 \times 3$ variables for profile data), while rows correspond to 247 cases (247 persons).
The reduction is possible due to symmetry and low kurtosis of data.

2.2.2. Principal components

The second reduction of data uses the principal components method. The columns are highly correlated, so the reduction is significant. The number of retained components depends on chosen level of explained variability 95%. The principal components are calculated from covariance matrix for ATN data, and from correlation matrix for RIT data.

The reduction for ATN is substantial – from 114 to 25, for RIT from 54 to 17; for RITx – from 27 to 9.

2.2.3. Classification

The classification is provided in two steps:

- Hierarchical clustering using k-means method on the reduced data (principal components step),
- Classification tree on data after first reduction (frequencies × quantiles) using classes obtained in first classification step.

The second step provides a better description of the classes showing which frequencies and which quantiles are responsible for classification. It is interesting that in classification only the first and third quartile is used. It means that in classification the greatest influence have the tails of distribution, not the central tendency parameters, as often believed.

2.2.3.1. *ATN classification*. Hierarchical clustering shows that the data is not homogenous. It is possible to divide the data into two or three clusters. The ANOVA comparison between the system with two clusters and system with three clusters shows that the system with three clusters is significantly better (Fig. 5). The ANOVA tests show that only the first principal component gives statistically significant differences between the groups. To find the outliers the distance between cluster centers and each member of cluster was calculated. Seven persons are the outliers in the classification of ATN measurements.

2.2.3.2. *RIT classification*. The file RIT includes the RIT and amplitude data for nine frequency pairs. Hierarchical clustering shows that the data are not homogenous. The ANOVA comparison between the system with two clusters and system with three clusters shows that the system with two clusters is significantly better (Fig. 6). The ANOVA tests show that only the first principal component gives statistically significant differences between the groups. Four persons are the outliers in the classification of RIT measurements.

2.2.3.3. *RITx classification*. The set RITx includes the RIT data for nine frequency pairs. Hierarchical clustering shows that the data is not homogenous. The ANOVA comparison between the system with two clusters and system with three clusters shows that the system with two clusters is significantly better (Fig. 6). The ANOVA tests show that only the second principal component gives statistically significant differences between the groups. Five persons are the outliers in the classification of RITx measurements.

2.2.4. Comparison of clusters

The Chi-square test was provided to compare the clusters between the different measurements. The test shows that the clusters of RIT and ATN are highly correlated:

- the class 1 of RIT correlate with class 2 of ATN;
- the class 2 of RIT correlate with class 3 of ATN.

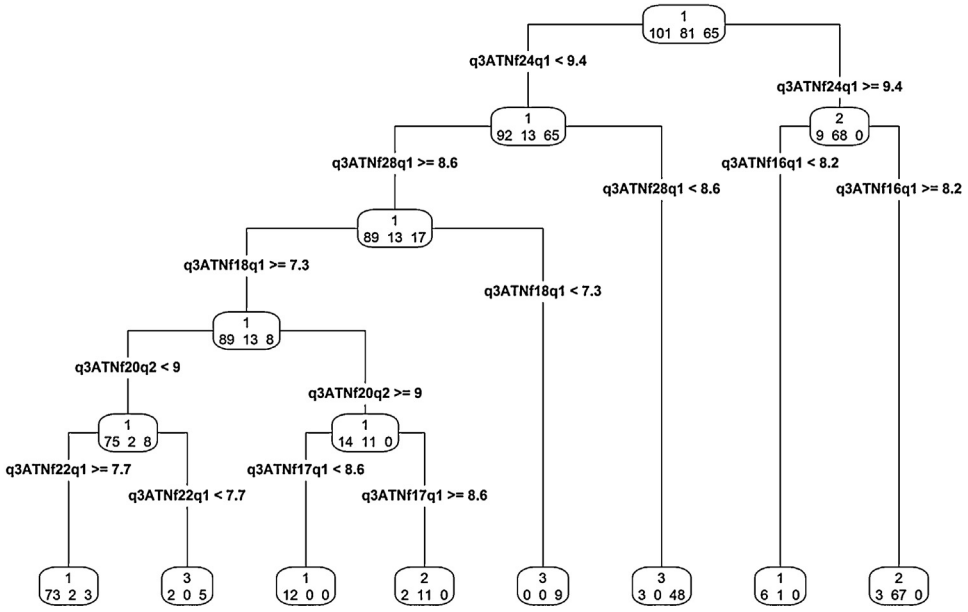

Fig. 5 – Classification Tree for ATN: each branch contains an attribute test condition to separate cases that have different characteristics. The nodes enclose two kinds of information: the upper row contains the classification suggestion; the lower one determines frequencies of individuals in each of the considered classes.

2.3. *Correlation of additional features with ATN, RIT and RITx classification*

The dependence of classification modalities and factor levels was verified by exact Fisher test.[1] The strength of relation between specific classification modality and factor level is described by standardized residuals (Pearson residuals).

For a contingency table $[n_{ij}]$, where n_{ij} is the number of cases in class i and feature level j the *standardized Pearson residual* is the value

$$r_{ij} = \frac{n_{ij} - e_{ij}}{\sqrt{(1-p_i)(1-q_j)e_{ij}}} \tag{6}$$

where

$$e_{ij} = \frac{n_{i+} \cdot n_{+j}}{n},\ n_{i+} = \sum_j n_{ij},\ n_{+j} = \sum_i n_{ij},\ n = \sum_{ij} n_{ij},\ p_i = \frac{n_{i+}}{n},\ q_j = \frac{n_{+j}}{n} \tag{7}$$

The positive values of the residual indicate over-representation of the feature in the class. The negative value of the residual indicate the significant under-representation of the feature in the class. The Pearson residuals are known as significant if $|r_{ij}| \geq 1.96$.

2.3.1. *Class characteristics*

In Tables 1–3 classes are described by *statistically significantly dependent* features (upper table) and, in the case of nonsignificant dependence, by features which have significant Pearson residuals. The features are expressed in interval continuous scale or as the factors.

- For features in continuous scale the classes are described by mean value and, in the case of ATN classification, by grouping variable (A, B).
- For factor features the strength is described by standardized residuals (Pearson residuals). The positive values of residuals indicate the significant over-representation of the future in the class. The negative values of residuals indicate the significant under-representation of the future in the class.
- The strength of binary (dichotomic) feature is preceded by letters: T(rue) if the future exists or F(alse) if the future did not exists in the class.
- The strength of multiple level feature is preceded by the digit, representing the level of the feature.

The ATN class 1 is significantly correlated with mean age of 40.3 years, occurrence of stroke in the grandparents, non-abstinence and occurrence of infarct in parents.

The ATN class 2 is significantly correlated with mean age of 46.8 years, nonoccurrence of stroke in the grandparents, never drinking wine, abstinence and nonoccurrence of infarct in parents.

The ATN class 3 is significantly correlated with mean age of 38.1 years.

In conclusion:

- The ATN class 1 is significantly correlated with the people who have some problems in their family history (e.g. stroke, infarct) and who are non-abstinence.
- The ATN class 2 is significantly correlated with the people without any problems with abstinence or family history problems (e.g. stroke, infarct).

[1] If the cardinalities in contingency table are small the Fisher test is more appropriate.

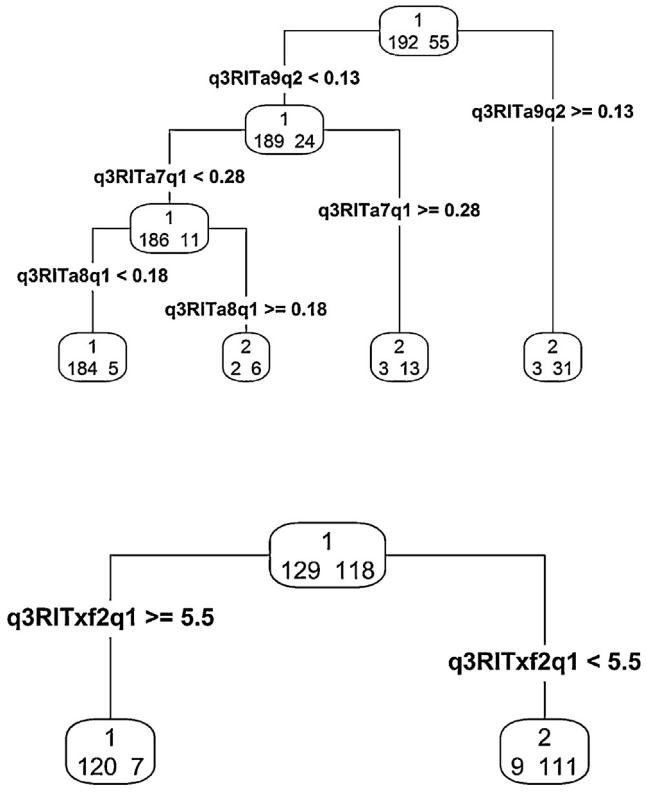

Fig. 6 – Classification Tree for RIT and RITx: each branch contains an attribute test condition to separate cases that have different characteristics. The nodes enclose two kinds of information: the upper row contains the classification suggestion; the lower one determines frequencies of individuals in each of the considered classes.

Observing the significant Pearson residuals, one can conclude that:

- The ATN class 1 is related with non-obese people (BMI class 4).
- The ATN class 2 is related with people who never drink beer, vodka, smoke 5–10 cigarettes per week and finished high school.

The RIT class 1 is significantly correlated with mean age 43.7 years, mean weight 74.4 kg, mean BMI value 25.4, with the people who have higher than primary education, with the nonoccurrence of infarct in their grandparents, but with the significant occurrence of thyroid.

The RIT class 2 is significantly correlated with mean age 34.9 years, mean weight 68.0 kg, mean BMI value 23.6, with the people who have primary education, with the occurrence of infarct in their grandparents, but with the significant nonoccurrence of thyroid.

Observing the significant Pearson residuals, one can conclude that:

The RIT class 1 is related with the group of people who smoke 0–5 cigarettes per week, while the RIT class 2 is related with the group of people who smoke more than 5 cigarettes per week

The RITx class 1 is significantly correlated with mean weight 75 kg and BMI value 25.6, while the RITx class 2 is significantly correlated with mean weight 71.1 kg and BMI value 24.4.

All calculations were performed on Open Source environment R version 3.1.1 Copyright (C) 2014 The R Foundation for Statistical Computing.

Table 1 – ATN classification characteristics; p is the p-value of exact Fisher test.

ATN class	Age* $p < 0.001$	Stroke grandparents* $p = 0.006$	Drinkwine* $p = 0.02$
1	40.3 B	T 2.41	
2	46.8 A	F 2.89	0: 3.24; 1: −2.96
3	38.1 B		
ATN class	**Abstinent*** $p = 0.04$	**Infarct parents*** $p = 0.05$	**Drink beer** $p = 0.14$
1	F 1.97	T 2.40	
2	T 2.49	F 1.95	0: 2.52; 1: −2.45
3			
ATN class	**BMI class** $p = 0.16$	**Drink vodka** $p = 0.22$	**Education** $p = 0.23$
1	4: −1.97		
2		0: 2.52; 1: −2.45	2: 2.14

* Statistically significant correlation.

Table 2 – RIT classification characteristics; upper table – significant ($p \leq 0.05$) dependence; p is the p-value of exact Fisher test.

RIT class	Age* $p < 0.001$	Weight* $p = 0.006$	BMI* $p = 0.009$	Education* $p = 0.01$
1	43.7	74.4	25.4	1: −3.10
2	34.9	68.0	23.6	1: 3.10

RIT class	Infarct grandparents* $p = 0.05$	Thyroid* $p = 0.05$	Smoke $p = 0.12$
1	F 2.07	T 2.11	0–5: 1.96
2	T 2.07	F 2.11	0–5: −1.96

* Statistically significant correlation.

Table 3 – RITx classification characteristics; p is the p-value of exact Fisher test.

RITx class	Weight* $p = 0.04$	BMI* $p = 0.03$	Stroke parents* $p = 0.007$	Education $p = 0.07$	Smoke $p = 0.16$
1	75.0	25.6	T 2.84	2: 2.31	5–10: −2.21
2	71.1	24.4	F 2.84	2: −2.31	5–10: 2.21

* Statistically significant correlation.

3. Conclusions

None of the volunteers that were considered in the control group had any identified stroke symptoms or congestion. However, the ultrasonic test indicated that there is no homogeneous but rather heterogeneous group to this respect (see RITx classification tree (Fig. 6). *High* **BP** (*blood pressure*), TIA (*transient ischemic attack*), *focal symptoms of weakness or speech impairment*, age, gender, diabetes mellitus, current cigarette smoking, diabetes, high BMI, heart disease. All the symptoms cited above (except three highlighted in italics) were shown in our study. We observed that a group of almost 39% respondents was distinguished by our multispectral ultrasonic testing (CAMUD). The respondents in this group have the minimum value of ATN for 17, 18, 22, 24 and 28. frequency higher than others. Intriguing, these values are almost perfectly correlated with the risk of stroke factors indicated in Russo et al. [1]; Lloyd-Jones et al. [2]; Medscape [3]. Namely: *age, increased alcohol consumption, cases of heart disease and stroke in the family* was over-proportionally represented by this group. Our investigations clearly show the potential of the CAMUD as a very powerful diagnostic method to detect and quantify a persons' risk of stroke, based on analyzing that person's brain tissue health, using non-invasive multispectral ultrasonic brain measurements and adaptive profiles.

4. Further investigations

The purpose of future study is the implementation of CAMUD to detect a cryptogenic stroke, microangiopathic white lesions (WML) and cerebral microbleeds (CMB) in comparison to MRI imaging of patients with atrial fibrillation (AF) who are treated with chronic anticoagulation. Independently, we would like to find a correlation between the CAMUD signals and diagnostic method and certain clinical outcomes including symptomatic stroke, dementia, depressive symptoms and cognitive disorder in patients with AF during a 5 year period. We would like to include in our study 50 patients aged over 65 years with AF (control group will be 30 patients without AF). We selected patients with AF because in the last 20 years, AF has become one of the most important public health problems and a significant cause of increasing health care costs in western countries. The prevalence of AF is increasing due to our greater ability to treat chronic cardiac and non-cardiac diseases, and the improved ability to suspect and diagnose AF. At the present time, the prevalence of AF (2%) is double than that reported in the last decade. The prevalence of AF varies with age and gender. AF is present in 0.12–0.16% of those younger than 49 years, in 3.7–4.2% of those aged 60–70 years, and in 10–17% of those aged 80 years or older. It has been approximated that 2.2 million people in the North America and 4.5 million in European Union have paroxysmal or persistent atrial fibrillation. AF itself is an independent long-term risk factor of stroke and related cardio-embolic cerebrovascular accidents. Moreover, it is sometimes overlooked that silent ischemic stroke (SS) is frequently seen in patients with asymptomatic AF [7–15]. Although present knowledge and MRI-associated costs do not support routine use of brain MRI in asymptomatic patients with AF, as more data emerge MRI may become an increasingly useful way to stratify patients with AF and individualize their treatment. We are going to compare magnetic resonance imaging (MRI) of the brain with

the CAMUD signals and diagnostic method in patients with AF treated with chronic anticoagulation.

Financial support

Hereby we inform that our financial supporters are:

1 Development Bank of Saxony, Pirnaische Straße 9, 01069 Dresden, Germany.
2 SoNovum, Perlickstrasse 5, 04103 Leipzig, Germany.

The funders exhibit no role in the collection, analysis and interpretation of data.

Conflicts of interests

Data acquisition for this study was supported by research grants from SonoMED Sp. Z o.o. to the clinical sites. Anna Olak-Popko, MD, as well as Dr. Robert Olszewski, MD, were a principal investigators at one of the clinical data acquisition sites at the time of this study. Mr. Miroslaw Wrobel serves as a CTO to SoNovum AG and holds potential financial interest through patented technology licensed by SoNovum from NimTECH, Inc.. SoNovum AG had no role in the conduct of the studies but partially by analysis of the data and preparation of manuscripts. Strict adherence to ethical concerns was followed and all subjects signed written informed consent forms for participation in the study.

Acknowledgements

SoNovum AG wants to express its deep gratitude to the Development Bank of Saxony (SAB) with all its attention for supporting our efforts in fundamental research and developing of this new diagnostic method, ECHO II, with EFRE Grant No. 100109012/990.301573.3.

REFERENCES

[1] Russo CA, Ho K, Elixhauser A. Hospital stays for circulatory diseases, 2004. Rockville, MD: Agency for Healthcare Research and Quality; February 2007.
[2] Lloyd-Jones D, Adams R, Carnethon M, De Simone G, Ferguson TB, Flegal K, et al. A report from the American Heart Association Statistics Committee and Stroke Statistics Subcommittee, Heart disease and stroke statistics – 2009 update.
[3] Medscape. New stroke prevention guidelines: a quick and easy guide; January 2015.
[4] Mazur R. Dynamics of brain density in the acute phase of ischemic stroke. Udar Mózgu 2002;4(1):1–8.
[5] O'Donnel M, Jayess ET, Miller JG. Kramers–Kronig relationship between ultrasonic attenuation and phase velocity. J Acoust Soc Am 1981;69(March (3)):1.
[6] Wrobel M. Advanced ultrasonic interferometer and method of non-linear classification and identification of matter using the same, WO 2007/000047, June 28, 2005.
[7] Zoni-Berisso M, Lercari F, Carazza T, Domenicucci S. Clin Epidemiol 2014;6:213–9.
[8] Haeusler KG, Wilson D, Fiebach JB, Kirchhof P, Werring DJ. Brain MRI to personalise atrial fibrillation therapy: current evidence and perspectives. Heart 2014;100(18):1408–13. http://dx.doi.org/10.1136/heartjnl-2013-305151 [Epub 2014 June 20]
[9] Bang OY, Ovbiagele B, Kim JS. Evaluation of cryptogenic stroke with advanced diagnostic techniques. Stroke 2014;45:1186–94.
[10] Saito T, Kawamura Y, Tanabe Y, Asanome A, Takahashi K, Sawada J, et al. Cerebral microbleeds and asymptomatic cerebral infarctions in patients with atrial fibrillation. J Stroke Cerebrovasc Dis 2014;23(July (6)):1616–22.
[11] Fisher M. MRI screening for chronic anticoagulation in atrial fibrillation. Front Neurol 2013;4(Oct):137.
[12] Kobayashi A, Iguchi M, Shimizu S, Uchiyama S. Silent cerebral infarcts and cerebral white matter lesions in patients with nonvalvular atrial fibrillation. J Stroke Cerebrovasc Dis 2012;21:310–7.
[13] Gage BF, Waterman AD, Shannon W, Boechler M, Rich MW, Radford MJ. Validation of clinical classification schemes for predicting stroke: results from the National Registry of Atrial Fibrillation. JAMA 2001;285:2864–70.
[14] Tatu L, Moulin T, Bogousslavsky J, Duvernoy H. Arterial territories of human brain: brainstem and cerebellum. Neurology 1996;47(5):1125–35.
[15] Tatu L, Moulin T, Bogousslavsky J, Duvernoy H. Arterial territories of the human brain: cerebral hemispheres. Neurology 1998;50(6):1699–708.
[16] Jodlowski L. Pomiar fazy sygnalu harmonicznego z zastosowaniem niskich czestotliwosci próbkowania, Conference Materials, 27th Winter School on Molecular and Quantum Acoustics, Ustron 23–27/02/1998.
[17] Szostakowski M, Jodlowski L. Measurements of changes of phase velocity in a fluid using digital. 27th Winter School on Molecular and Quantum Acoustics, Ustron (Poland) February 1998.